Liquid-crystal pumping in a cylindrical capillary with radial temperature gradient

A. V. Zakharov* and A. A. Vakulenko†
Saint Petersburg Institute for Machine Sciences, The Russian Academy of Sciences, Saint Petersburg 199178, Russia
(Received 27 May 2009; published 18 September 2009)

Dynamic field pumping principle has been developed utilizing the interactions of both the director and velocity fields and a temperature gradient ∇T. The orientational dynamics in the hybrid-oriented liquid-crystal (HOLC) microvolume confined between two infinitely long coaxial cylinders under the influence of the radially directed ∇T has been investigated. We have carried out a numerical study of a system of hydrodynamic equations including director reorientation, fluid flow, and temperature redistribution across the HOLC cavity between two cylinders under the influence of ∇T, when the liquid-crystal cavity is heated both from outer (inner) to inner (outer) bounding cylinders. Calculations show that under the influence of ∇T the initially quiescent HOLC drop settles down to a stationary flow regime, with the horizontal $u_{st}(r)$ component of velocity. The effects of ∇T, of the character of the preferred anchoring of the average molecular direction to the restricted cylinders, and of the size of the HOLC cavity on magnitude and direction of hydrodynamic flow—for a number of hydrodynamic regimes—has been investigated.

DOI: 10.1103/PhysRevE.80.031708 PACS number(s): 61.30.Cz, 65.40.De

A trend toward miniaturization in the drug delivery devices, medical diagnostics, manipulation of biomolecules, and biosensing has brought an increasing number of integrated microdevices for chemical and biological applications. These are known as micrototal analysis systems or biological lab-on-a-chip systems [1]. Manipulation of these systems can be realized by various kinds of external perturbations (pressure, temperature, electric, or/and magnetic fields). Such a manipulation, for instance, of flow can be achieved either by forces applied macroscopically, e.g., at appropriate inlets or outlets, or can be generated locally within the microchannel or liquid-crystal (LC) cell [2]. A challenging problem in all such systems is the precise handling of LC or isotropic liquid microvolume, which in turn requires self-contained micropumps of small package size exhibiting either a very small displacement volume (displacement pumps [2]) or a continuous volume flow (dynamic pumps [2]). Different dynamic field pumping principles have been developed based on interactions of the fluid with an electric and/or magnetic field. For instance, electrokinetics is now studied in a variety forms for controlling microflows. Electro-osmosis, where the field moves relative to stationary charged boundaries [3], dielectrophoresis, which moves an interface in a gradient electric field [4], and electrowetting, where the electric field modifies wetting properties [5], all have been exploited.

Alternatively, when a gas-liquid interface is present, fluid motion can also be generated by controlling spatial variations of surface tension (the so-called Marangoni stresses). These variations can be created with thermal, electrical, light, and capillary pressure gradients. It is also possible to move the LC-gas menisci in channels or capillaries by using thermal gradients.

Recently, the problem of horizontal motion of an ultrathin (a few micrometers) LC drop placed between two horizontal plates, and subjected to uniform heating both from below or above, has attracted attention [6–9]. In the case of a hybrid-oriented LC (HOLC) cell, of thickness d, it has been shown that, in the heat conduction regime, the magnitude of the hydrodynamic flow v excited by a temperature gradient ∇T is $v \sim \frac{d}{\eta}\sigma_{zx}^{tm}$, where η denotes the viscosity, $\sigma_{zx}^{tm} \sim \xi(\Delta T/d^2)$ is the tangential component of the thermomechanical stress tensor (ST) σ_{ij}^{tm}, and ξ is the thermomechanical constant. Here, $\Delta T = T_2 - T_1 > 0$ is the temperature difference across the LC cell boundaries, and the range $[T_2, T_1]$ still falls within the stability region of the nematic phase. The direction of hydrodynamic flow $\mathbf{v}$ is influenced by both the direction of heat flow and the character of the preferred anchoring of the average molecular direction $\hat{\mathbf{n}}$ on the bounding surfaces [6,9]. On the other hand, in LC cells where director anchorings on the two bounding surfaces are the same, i.e., both strongly homeotropic or homogeneous, the LC microvolume remains quiescent under the influence of the temperature gradient.

It should be pointed out that the thermally driven convection in a millimeter-sized horizontal layer of a nematic LC heated below or above and in a magnetic field has been studied for approximately 40 years [10,11]. At such scales a number of hydrodynamic instabilities in LCs subjected to the steady thermal gradient can take place [11].

The objective of this paper is to analyze the response of the nematic LC confined in the microvolume between two horizontal coaxial cylinders under the influence of the temperature gradient ∇T directed from the inner (outer) cooler (warmer) to outer (inner) warmer (cooler) cylinders. So, we are primarily concerned here with describing the way how the temperature gradient across the microvolume cavity between two coaxial cylinders can produce the hydrodynamic flow. It will be treated in the framework of the classical Ericksen-Leslie theory [12,13], together with accounting for the thermoconductivity equation for the temperature field [14]. To fix ideas and notation, we shall be considering a HOLC system composed of asymmetric polar molecules, such as *cyanobiphenyls*, at the density ρ and confined be-

*Author to whom correspondence should be addressed. avz02@yahoo.com; www.ipme.ru/~zakharov
†avak2vale@mail.ru; www.ipme.ru/~vakulenko

tween two infinitely long horizontal coaxial cylinders with radii R_1 and R_2 ($R_1 < R_2$) that impose a preferred orientation of the average molecular direction $\hat{\mathbf{n}}$ on both bounding surfaces, for instance, homeotropic on the inner cooler ($T_{\text{in}}=T_1$), and planar, on the outer warmer ($T_{\text{out}}=T_2$) bounding cylinders. So, one deals with the HOLC system under the influence of the radially directed temperature gradient ∇T parallel to the unit cylindrical vector $\hat{\mathbf{e}}_r$ along the radius r. The coordinate system defined by our task assumes that the director $\hat{\mathbf{n}}$ lies in the rz plane, where $\hat{\mathbf{e}}_z$ is the unit vector which coincides with the planar director orientation, for instance, on the outer warmer (inner cooler) bounding cylinder ($\hat{\mathbf{e}}_z \| \hat{\mathbf{n}}_{r=R_2(=R_1)}$), where $\hat{\mathbf{e}}_r$ denotes the unit vector along the radius r and $\hat{\mathbf{e}}_\varphi = \hat{\mathbf{e}}_z \times \hat{\mathbf{e}}_r$ is the tangential unit vector.

Note that a horizontal ultrathin (micrometer-sized) LC layer, being initially at rest and heated both from below or above, starts moving in the horizontal direction due to the temperature gradient [6,8,9], but only when the anchorings on the two bounding surfaces are different. This gradient, if expressed in suitable dimensionless units, is called the Rayleigh ($\mathcal{R}$) number. As long as the Rayleigh number is not too large, heat is transported by conduction [15]. It should be pointed out that a thin (millimeter-sized) horizontal layer of quiescent LC fluid heated from below becomes unstable to convection via the Rayleigh-Bénard mechanism; this instability occurs at a value $\mathcal{R}=\mathcal{R}_c \sim 1708$ independent of the fluid under consideration [15]. Taking into account that the size of the LC cavity $d \equiv R_2 - R_1$ is $\sim 5-10$ μm, in our case $\mathcal{R} \ll \mathcal{R}_c$, and the driving force is not strong enough to produce convection via the Rayleigh-Bénard mechanism; thus, in the following we shall be focusing primarily on the heat conduction regime for the HOLC system. Assuming that the temperature gradient ∇T varies only in the r direction, $\nabla T = \frac{\partial T(t,r)}{\partial r}\hat{\mathbf{e}}_r$, and the director $\hat{\mathbf{n}}$ belongs to the rz plane, in the case of the infinitely long cylinders we can suppose that the components of the director $\hat{\mathbf{n}} = \sin\theta(t,r)\hat{\mathbf{e}}_r + \cos\theta(t,r)\hat{\mathbf{e}}_z$, as well as the rest of the relevant physical quantities, only depend on the radius r and on time t. Here, θ denotes the angle between the direction of the director $\hat{\mathbf{n}}$ and the unit vector $\hat{\mathbf{e}}_z$ directed parallel to the long cylinder's axis. Moreover, we will assume homeotropic and homogeneous strong anchoring conditions on the outer and inner cylinders,

$$\theta(r)_{r=R_2} = 0, \quad \theta(r)_{r=R_1} = \frac{\pi}{2}, \tag{1}$$

and no-slip boundary conditions for the nematogenic molecules on both bounding cylindrical surfaces, i.e.,

$$v(r)_{r=R_1} = v(r)_{r=R_2} = 0, \tag{2}$$

respectively. Upon assuming an incompressible fluid $\nabla \cdot \mathbf{v} = 0$, the hydrodynamic equations describing the reorientation of the hybrid aligned nematic system confined in the microvolume between two horizontal coaxial cylinders under the influence of the temperature gradient ∇T directed from the inner cooler to outer warmer cylinders,

$$T(r)_{r=R_1} = T_{\text{in}}, \quad T(r)_{r=R_2} = T_{\text{out}}, \tag{3}$$

can be derived from the balance of elastic, viscous, and thermomechanical torques $\mathbf{T}_{\text{el}} + \mathbf{T}_{\text{vis}} + \mathbf{T}_{\text{tm}} = 0$; the Navier-Stokes equation for the velocity field $\mathbf{v}$, excited by ∇T; and the equation for heat conduction. Here, $\mathbf{T}_{\text{el}} = (\delta W_{\text{F}}/\delta \hat{\mathbf{n}}) \times \hat{\mathbf{n}}$, $\mathbf{T}_{\text{vis}} = (\delta \mathcal{R}_{\text{vis}}/\delta \dot{\hat{\mathbf{n}}}) \times \hat{\mathbf{n}}$, and $\mathbf{T}_{\text{tm}} = (\frac{\delta \mathcal{R}_{\text{tm}}}{\delta \dot{\hat{\mathbf{n}}}}) \times \hat{\mathbf{n}}$, where $\dot{\hat{\mathbf{n}}} = \frac{d\hat{\mathbf{n}}}{dt}$ is the material derivative of the director $\hat{\mathbf{n}}$, $W_{\text{F}} = \frac{1}{2}[K_1(\nabla \cdot \hat{\mathbf{n}})^2 + K_3(\hat{\mathbf{n}} \times \nabla \times \hat{\mathbf{n}})^2]$ is the elastic energy, K_1 and K_3 are splay and bend elastic constants, and $\mathcal{R} = \mathcal{R}_{\text{vis}} + \mathcal{R}_{\text{tm}} + \mathcal{R}_{\text{th}}$ is the full dimensionless Rayleigh dissipation function composed by the viscous, thermomechanical, and thermal contributions, respectively. The incompressibility condition,

$$\nabla \cdot \mathbf{v} = \frac{1}{r}\frac{\partial [r v_r(t,r)]}{\partial r} + \frac{\partial v_z(t,r)}{\partial z} = \frac{1}{r}\frac{\partial [r v_r(t,r)]}{\partial r} = 0,$$

together with the no-slip condition (2) implies the existence of only one nonzero component for the vector $\mathbf{v}$, viz., $\mathbf{v}(t,r) = v_z(t,r)\hat{\mathbf{e}}_z \equiv u(t,r)\hat{\mathbf{e}}_z$. In the cylindrical coordinate system the dimensionless torque balance equation takes the form [6,9,16]

$$\bar{\gamma}_1(\chi)\theta_\tau = \mathcal{A}(\theta)u_r + [\mathcal{G}(\theta)\theta_r]_r - \frac{1}{2}\mathcal{G}_\theta(\theta)\theta_r^2 + \frac{\theta_r}{r}\mathcal{G}(\theta) + \frac{1}{2}\left(\frac{\bar{K}_1(\chi)}{r}\right)_r - \delta_1\chi_r\left[\theta_r\left(\frac{1}{2} + \cos^2\theta\right) + \frac{3}{4r}\sin 2\theta\right], \tag{4}$$

where $\bar{\gamma}_1 = \gamma_1(\chi)/\gamma_{10}$, $\theta_\tau = \frac{\partial\theta(\tau,r)}{\partial\tau}$, $\theta_r = \frac{\partial\theta(\tau,r)}{\partial r}$, $u_r = \frac{\partial u(\tau,r)}{\partial r}$, $\mathcal{A}(\theta) = -(1/2\gamma_{10})[\gamma_1(\chi) + \gamma_2(\chi)u_r(\tau,r)\cos 2\theta]$ and $\mathcal{G}(\theta) = [K_1(\chi)/K_{10}]\sin^2\theta + [K_3(\chi)/K_{10}]\cos^2\theta$ are the hydrodynamic and elastic functions, $\chi(\tau,r) = T(\tau,r)/T_{\text{NI}}$ is the dimensionless temperature, and T_{NI} is the nematic-isotropic transition temperature. Here, γ_{10} and K_{10} are the highest values of the rotational viscosity coefficient $\gamma_1(\chi)$ and of the splay constant $K_1(\chi)$ in the temperature interval $\Delta\chi = \chi_2 - \chi_1$ belonging to the nematic phase, $\chi_1 = T_1/T_{\text{NI}}$, $\chi_2 = T_2/T_{\text{NI}}$, $\tau = (K_{10}/\gamma_{10}d^2)t$ is the dimensionless time, and $\bar{r} = \frac{r}{d}$ is the dimensionless radius.

Notice that the overbars in the space variable r have been (and will be) eliminated in the last as well as in the following equations. In the case of incompressible fluid, the dimensionless Navier-Stokes equation (in cylindrical coordinates) takes the form [6,8,16]

$$\delta_2 u_\tau = \nabla_r \cdot \sigma_{rz}, \tag{5}$$

where $\delta_2 = \rho K_{10}/\gamma_{10}^2$ is an additional parameter of the system, $\nabla_r \cdot \sigma_{rz} = \partial\sigma_{rz}/\partial r + \sigma_{rz}/r$, and $\sigma_{rz} = \partial\mathcal{R}/\partial u_z$ is the tangential ST σ_{ij} $(i,j = r,z)$ component. Here, $\mathcal{R}(\tau,r) = (\gamma_{10}d^4/K_{10})\mathcal{R}(t,r)$ is the full dimensionless Rayleigh dissipation function, where $\mathcal{R}(t,r) = \mathcal{R}_{\text{vis}} + \mathcal{R}_{\text{tm}} + \mathcal{R}_{\text{th}}$, and $\mathcal{R}_{\text{vis}} = \frac{1}{2}[\gamma_1\theta_t^2 + u_r\theta_t\bar{\mathcal{A}}(\theta) + h(\theta)u_r^2]$ is the viscous, $\mathcal{R}_{\text{tm}} = \xi T_r[\theta_t\theta_r(\frac{1}{2} + \cos^2\theta) + \frac{1}{4r}\theta_t\sin 2\theta + u_r\mathcal{H}(\theta)]$ is the thermomechanical, and $\mathcal{R}_{\text{th}} = (T_r^2/2T)(\lambda_\parallel \sin^2\theta + \lambda_\perp \cos^2\theta)$ is the thermal contribution,

respectively. Here, $\overline{\mathcal{A}}(\theta)=\gamma_{10}\mathcal{A}(\theta)$, $4h(\theta)=2\gamma_1(T)+\alpha_5(T)+\alpha_6(T)+2\alpha_4(T)+2\gamma_2(T)\cos 2\theta+\alpha_1(T)\sin^2 2\theta$, and $\mathcal{H}(\theta)=\theta_r\cos^2\theta(1+\frac{1}{2}\sin^2\theta)+\frac{3}{4r}\sin 2\theta$ are hydrodynamic functions; $\alpha_i(T)$ $(i=1,\ldots,6)$ are the six temperature-dependent Leslie coefficients; and $\lambda_\parallel$ and $\lambda_\perp$ are the heat conductivity coefficients parallel and perpendicular to the director $\hat{\mathbf{n}}$. When a small temperature gradient ∇T (in our case ~ 0.1 K/μm) is set up across the cavity between two infinitely long coaxial cylinders, we expect the temperature field $\chi(\tau,r)$ to satisfy the dimensionless heat conduction equation

$$\delta_3\chi_\tau=\frac{1}{r}[r\chi_r(\lambda\sin^2\theta+\cos^2\theta)]_r + \delta_4\frac{1}{r}\left\{r\chi\left[\theta_\tau\theta_r\left(\frac{1}{2}+\cos^2\theta\right)+\frac{\theta_\tau}{4r}\sin 2\theta + u_r\frac{\mathcal{H}(\theta)}{d}\right]\right\}_r, \tag{6}$$

where $\lambda=\lambda_\parallel/\lambda_\perp$, $\delta_3=\rho C_p K_{10}/(\lambda_\perp\gamma_{10})$, and $\delta_4=\xi K_{10}/(\lambda_\perp\gamma_{10}d^2)$ are the two additional parameters of the system and C_p is the heat capacity. The above-mentioned hybrid anchoring conditions for the director $\hat{\mathbf{n}}$ now read

$$\theta_{r=a}=\frac{\pi}{2},\quad \theta_{r=a+1}=0, \tag{7}$$

$$\theta_{r=a}=0,\quad \theta_{r=a+1}=-\frac{\pi}{2}, \tag{8}$$

whereas the velocity on these cylinders has to satisfy the no-slip boundary condition

$$u(r)_{r=a}=u(r)_{r=a+1}=0. \tag{9}$$

As for the temperature field $\chi(\tau,r)$, the corresponding boundary conditions read

$$\chi_{r=a}=\chi_1,\quad \chi_{r=a+1}=\chi_2, \tag{10}$$

$$\chi_{r=a}=\chi_2,\quad \chi_{r=a+1}=\chi_1, \tag{11}$$

respectively. Here, $a=R_1/(R_2-R_1)$ is the dimensionless size of the HOLC cavity.

Notice that our approach is only valid for the nematic phase. For the case of 4-*n*-pentyl-4′-cyanobiphenyl (5CB), at temperature corresponding to the nematic phase, the parameters involved in Eqs. (4)–(6) are $\delta_1\sim 32$, $\delta_2\sim 10^{-6}$, $\delta_3\sim\times 10^{-3}$, and $\delta_4\sim 10^{-13}$ (for details, see [6]). Using the fact that δ_2, δ_3, and $\delta_4\ll 1$, both the Navier-Stokes (5) and the heat conduction (6) equations can be considerably simplified. Thus, the whole left-hand side of Eqs. (5) and (6) can be neglected, reducing it to

$$\sigma_{rz}=\frac{\mathcal{C}(\tau)}{r}, \tag{12}$$

$$[r\chi_r(\lambda\sin^2\theta+\cos^2\theta)]_r=0, \tag{13}$$

where the function $\mathcal{C}(\tau)$ does not depends on r and will be fixed by the boundary condition (9). The last equation has a solution

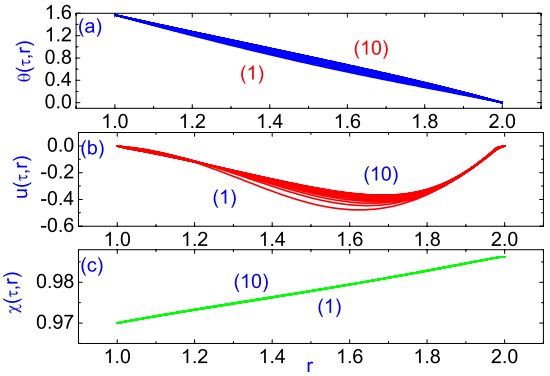

FIG. 1. (Color online) (a) Plot of the angle $\theta(\tau,r)$ across the LC cavity between two $a\le r\le a+1$ infinitely long coaxial hybrid-oriented [see Eq. (7)] cylinders, under the influence of the temperature gradient $\nabla\chi$, directed from the cooler inner ($T_{in}=0.97$) to warmer outer ($T_{out}=0.9862$) cylinders, at different times $\tau(k)=\frac{k}{10}\tau_R$ $(k=1,\ldots,10)$, whose values increase from curve (1) to curve (10). Here, $\tau_R=0.2$. (b) Same as (a), but the plot is that of the velocity $u(\tau,r)$ vs r. (c) Same as (a), but the plot is that of the temperature $\chi(\tau,r)$ vs r. All calculations were carried out for $a=1.0$.

$$\chi(\tau,r)=\frac{\Delta\chi}{\mathcal{I}}\int_a^r\frac{dr}{r(\lambda\sin^2\theta+\cos^2\theta)}+\chi_i, \tag{14}$$

where $\mathcal{I}=\int_a^{a+1}dr/[r(\lambda\sin^2\theta+\cos^2\theta)]$ and χ_i $(i=1,2)$.

The relaxation of the director $\hat{\mathbf{n}}$ to its equilibrium orientation $\hat{\mathbf{n}}_{eq}$, which is described by the angle $\theta(\tau,r)$, from the initial condition $\theta(\tau=0,a<r\le a+1)=\theta_{el}(r)$ to $\theta_{eq}(r)$ [see Fig. 1(a)], and velocity $u(\tau,r)=v_z(\tau,r)$ [see Fig. 1(b)], in the HOLC cavity, at different times ($\tau(1)=0.02$ (~ 1.4 s) [curve (1)] to $\tau(10)=\tau_R=0.2$ (~ 14 s) [curve (10)]), is shown in Fig. 1. In the studied case, the sample is heated from above with the dimensionless temperature difference $\Delta\chi=0.0162$ (~ 5 K). We solved the system of nonlinear partial differential equations (4), (12), and (14), together with the boundary conditions (7)–(11), by means of the numerical relaxation method [17]. Here, τ_R is the relaxation time of the system. In that case, the lower cooler surface is kept as constant equal to $\chi_1=0.97$ ($T_1\sim 298$ K). Note that the relaxation processes of the dimensionless temperature $\chi(\tau,r)$ to its equilibrium distributions $\chi_{eq}(r)$ across the HOLC cavity characterized practically the linear increasing of the values of $\chi(\tau,r)$, from χ_1 to χ_2 [see Fig. 1(c)]. In the calculations, the relaxation criterion $\epsilon=|[\theta_{(m+1)}(\tau,r)-\theta_{(m)}(\tau,r)]/\theta_{(m)}(\tau,r)|$ was chosen to be 10^{-4}, and the numerical procedure was then carried out until a prescribed accuracy was achieved. Here, m is the iteration number and τ_R is the relaxation time. According to our calculations, the relaxation processes of the dimensionless velocity $u(\tau,r)$ in the LC cavity between two infinitely long coaxial cylinders is characterized by the monotonic decrease in $|u(\tau,r)|$ upon increasing τ, before getting to the equilibrium distributions $u_{eq}(r)$ across the LC cavity. That distribution is characterized by the minimum near the middle part of the HOLC cavity, where the hydrodynamic flow is directed in the negative direction [see Fig. 2(a), curve (1)]. Note that the hydrodynamic flow $u_{eq}(r)$ change a direction, from the

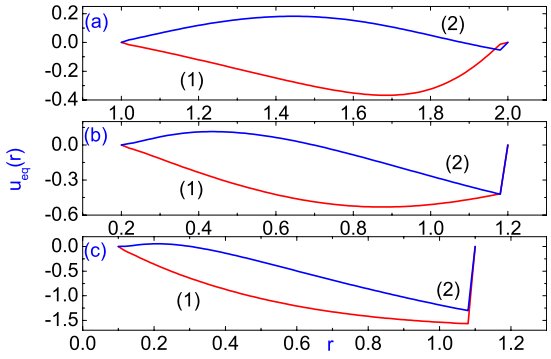

FIG. 2. (Color online) Dimensionless equilibrium velocity profile $u_{eq}(r)$ across the cavity between two $a \leq r \leq a+1$ infinitely long coaxial hybrid-oriented [see Eq. (7)] cylinders, under the influence of the radial temperature gradient $\nabla\chi$, directed from the cooler (warmer) inner χ_1 (χ_2) to warmer (cooler) outer χ_2 (χ_1) cylinders [see curves (1) and (2), respectively], calculated for a number of values of a: (a) 1.0, (b) 0.2, and (c) 0.1, respectively.

negative to positive sense, across the full thickness of the HOLC cavity, after changing of the temperature gradient $\nabla\chi$ direction, from the cooler (T_{in}=298 K) inner to the warmer outer (T_{out}=303 K) cylinders on the warmer (T_{in}=303 K) inner to the cooler outer (T_{out}=298 K) [see Fig. 2, curves (2)]. The maximum of the absolute magnitude of the dimensionless equilibrium velocity $u_{eq}(r)=(\gamma_{10}d/K_{10})v_z^{eq}(r)$, in the HOLC cavity between two infinitely long coaxial cylinders is equal to $\sim$2, in the vicinity of the warmer cylinder, at a=0.1 (R_2=11R_1) [see Fig. 3(c)].

It should be pointed out that increasing of the LC cavity size $d \equiv R_2 - R_1$ between two infinitely long coaxial cylinders, when the temperature gradient $\nabla\chi$ is directed from the inner to outer cylinders, leads to increase the maximum of the absolute magnitude of the dimensionless velocity $u_{eq}(r)$, from $u_{eq}^{max} \sim 0.4$ ($\sim$11 μm/s), at a=1 (R_2=2R_1), to $u_{eq}^{max} \sim 2$ ($\sim$55 μm/s), at a=0.1 (R_2=11R_1), respectively. According to our calculations, in the case when the hybrid-oriented anchoring conditions for director is described both by Eqs. (7) and (8), with $(\chi_1)_{r=a} > (\chi_2)_{r=a+1}$, one has arrived at the picture where the LC fluid settles down to the stationary flow regime in the negative verse (see Figs. 2 and 3). In the first case [Eq. (7)], the maximum of the velocity field

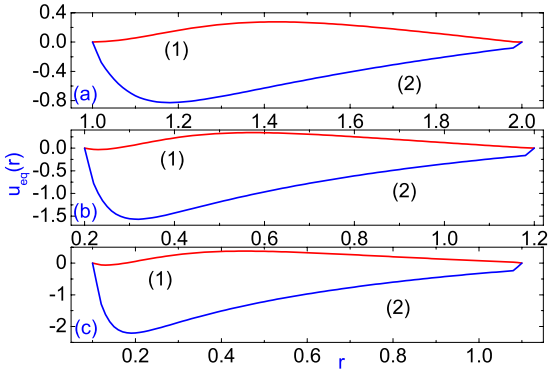

FIG. 3. (Color online) Same as Fig. 1, but the hybrid orientation is given by Eq. (8).

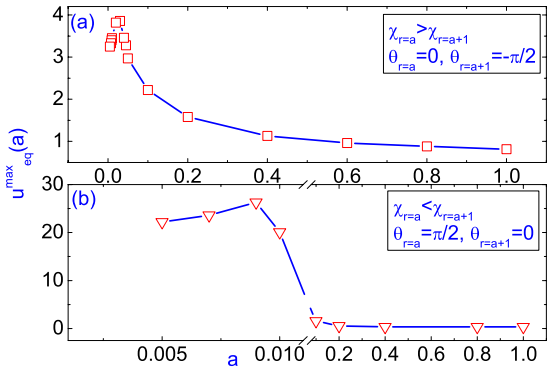

FIG. 4. (Color online) Dependence of $u_{eq}^{max}(a)$ on the size of the HOLC [Eq. (8)] cavity $a=R_1/(R_2-R_1)$, heated from inner to outer bounding cylinders.

$u_{eq}^{max}(r)$ is found in the vicinity of the cooler outer cylinder [see Fig. 2(c)], whereas in the second case [Eq. (8)], the maximum of $u_{eq}^{max}(r)$ is found in the vicinity of the warmer inner cylinder [see Fig. 3(c)], respectively. Physically, this means that the thermomechanical force may overcome the viscous and elastic forces and the LC drop confined between two infinitely long hybrid-oriented cylinders starts moving in the horizontal direction with the stationary distributed velocity profile across the LC cavity. So, we arrive at the picture where there is a balance between the applied temperature gradient and both the viscous and elastic forces and, in general, the LC fluid settles down to the stationary flow regime along the long cylinder's axis. The magnitude of the hydrodynamic flow u is proportional both to the tangential component of the thermomechanical ST σ_{rz}^{tm} and the cavity size R_2-R_1, and the direction of u is influenced by both the direction of the heat flow and the character of the preferred anchoring of the director on the restricted cylinders. The highest value of the dimensionless velocity $u_{eq}^{max}(r)$ is built up in the hybrid-oriented LC cavity, when the temperature gradient $\nabla\chi$ directed from the outer cooler (T_{out}=298 K) to inner warmer (T_{in}=303 K) cylinders, in the vicinity of the homogeneously oriented inner cylinder [see Eq. (8)], and equal to $\sim$2 ($\sim$55 μm/s) [see Fig. 3(c)], directed in the negative sense. The size of the HOLC cavity $a=R_1/(R_2-R_1)$ has a pronounced effect on the magnitude of $u_{eq}^{max}(a)$ (see Fig. 4). Figure 4(a) shows the effect of a on the magnitude of the highest dimensionless velocity $u_{eq}^{max}(a)$, when the temperature on the inner cylinder $(\chi)_{r=a}$ is greater than the temperature on the outer cylinder $(\chi)_{r=a+1}$. In the case a=0.03, i.e., when the radius of the outer cylinder $R_2 \sim 34R_1$, the maximum value of the dimensionless equilibrium velocity has the biggest value which is equal to $\sim$3.82 ($\sim$105 μm/s) and directed in the negative sense. Note that the further decrease in a leads to decreasing of the highest dimensionless velocity $u_{eq}^{max}(a)$. Figure 4(b) shows the effect of a on the magnitude of the highest dimensionless velocity $u_{eq}^{max}(a)$, in the case when $(\chi)_{r=a+1} > (\chi)_{r=a}$. Here, the biggest value is equal to $\sim$26 ($\sim$0.7 mm/s), at a=0.01 ($R_2 \sim 112R_1$), and $\Delta\chi$=0.0162 ($\sim$5 K) and directed also in the negative sense.

It should be noted here that the highest temperature difference $\Delta = T_{in(out)} - T_{out(in)}$ across the HOLC cavity is still

such that both T_{in} and T_{out} fall within the stability region of the nematic phase. The temperature difference, for instance, in ~5 K in the LC microvolume cavity confined between two infinitely long horizontal coaxial cylinders can be built up by using the laser-induced heating [18]. Indeed, since the laser beam can be focused to its diffraction limit, it can be used to inject energy at scales that are difficult to reach with other techniques.

In summary, we have investigated the relaxation of the director $\hat{\mathbf{n}}(t,\mathbf{r})$, velocity $\mathbf{v}(t,\mathbf{r})$, and temperature $T(t,\mathbf{r})$ in the HOLC microvolume cavity between two infinitely long coaxial cylinders to their equilibrium values, under the influence of the radial temperature gradient directed from the cooler to warmer bounding surfaces. Our calculations, based on the classical Ericksen-Leslie theory, show that, under the influence of the temperature gradient, the microvolume of HOLC material settles down to a stationary flow regime in the horizontal direction. It has been also shown that the magnitudes of the resulting velocity u is proportional to the tangential component of the ST σ_{rz}^{tm}, as well as to the size d of the LC cavity, and that the direction of $\mathbf{v}=u\hat{\mathbf{e}}_z$ is influenced by the magnitude of heat flow and the character of the preferred anchoring of the director on the bounding surfaces. Our calculations also show that the optimal pumping effect in the microvolume HOLC cavity between two coaxial cylinders build up under the influence of the radially applied temperature gradient, when $a=R_1/(R_2-R_1)\sim 0.01$, or when the radius of the homogeneously anchored warmer outer cylinder is greater than the radius of the homeotropically anchored cooler inner cylinder, approximately, by 100 times.

Notice that the above-mentioned flows are described by a continuous approach, where the length scales of the manipulated fluid, smaller than a few tens of micrometers, are reflected by the magnitudes of parameters δ_i $(i=1,2,3,4)$. It should be pointed out that the pumping effect under the influence of the radially directed thermal gradient is not found in the LC cavity when molecules are aligned homeotropically or homogeneously on both boundaries.

It is also worth noting that in the case of finite length of the LC cavity between two concentric cylinders $(z\sim r)$ with the hybrid bounding conditions for the director on the cylinder surfaces one should deal with a two-dimensional (2D) HOLC cavity, where all physical quantities also depend on the size z. In that case, the dissipation process in confined LC phase between two cylinders and two lateral bounding surfaces is characterized, for instance, by the hydrodynamic flow with the horizontal and vertical components, and the director redistribution takes place across the 2D HOLC cavity.

We believe that the precise handling of the liquid-crystal microvolumes can be developed utilizing the interactions of both the director and velocity fields with the radially directed temperature gradient [19]. Hence, the possible pumping technique described above appears applicable to various pumping strategies not involving mobile parts.

We acknowledge the financial support of the Russian Funds for Fundamental Research (Grant No. 09-02-00010-a).

[1] D. R. Reyes, D. Iossifidis, P. A. Auroux, and A. Mantz, Anal. Chem. **74**, 2623 (2002).
[2] H. A. Stone, A. D. Stroock, and A. Ajdari, Annu. Rev. Fluid Mech. **36**, 381 (2004).
[3] A. Ajdari, Phys. Rev. E **61**, R45 (2000).
[4] D. Long and A. Ajdari, Eur. Phys. J. E **4**, 29 (2001).
[5] M. Rauscher and S. Dietrich, Annu. Rev. Mater. Res. **38**, 143 (2008).
[6] A. V. Zakharov and A. A. Vakulenko, J. Chem. Phys. **127**, 084907 (2007).
[7] A. V. Zakharov and A. A. Vakulenko, Chem. Phys. Lett. **454**, 80 (2008).
[8] A. V. Zakharov, A. A. Vakulenko, and S. Romano, J. Chem. Phys. **128**, 074905 (2008).
[9] A. V. Zakharov and A. A. Vakulenko, Phys. Rev. E **79**, 011708 (2009).
[10] P. Pieranski, E. Dubois-Violette, and E. Guyon, Phys. Rev. Lett. **30**, 736 (1973).
[11] Guenter Ahlers, in *Pattern Formation in Liquid Crystals*, edited by A. Buka and L. Kramer (Springer, New York, 1996), pp. 165–221.
[12] J. L. Ericksen, Arch. Ration. Mech. Anal. **4**, 231 (1960).
[13] F. M. Leslie, Arch. Ration. Mech. Anal. **28**, 265 (1968).
[14] L. D. Landau and E. M. Lifshitz, *Fluid Mechanics* (Pergamon, Oxford, 1987).
[15] M. C. Cross and P. C. Hohenberg, Rev. Mod. Phys. **65**, 851 (1993).
[16] I. W. Stewart, *The Static and Dynamic Continuum Theory of Liquid Crystals* (Taylor and Francis, London, 2004).
[17] I. S. Berezin and N. P. Zhidkov, *Computing Methods*, 4th ed. (Pergamon Press, Oxford, 1965).
[18] M. L. Cordero, E. Verneuil, F. Gallaire, and Ch. N. Baroud, Phys. Rev. E **79**, 011201 (2009).
[19] A. D. Rey, Soft Matter **3**, 1349 (2007).